CHAPTER 4

Results and Discussion

Our data are composed of 20 images containing more than 3500 WBCs. More than 1400 cells correspond to CD4+ lymphocytes. The input images size is 1200 x 1600 pixels which are captured under 20x objective lens with various illumination. The detection results of proposed algorithm are compared to the manual detection by 3 experts, medical technologist whom professional with this field, for performance evaluation. The algorithm result and discussion of WBCs detection will be described first, then following by CD4+ lymphocyte detection.

4.1 WBCs Detection

As mentioned earlier that CD4+ lymphocyte is a type of WBC. The aim of detecting WBCs in bright field image is to address the position where the CD4+ lymphocytes possibly locate. Conceptually, the more WBCs are detected, the possibility to detect CD4+ lymphocytes increase. However, our bright field images contain some difficulty. Besides WBCs, the unwanted objects such as red blood cells (RBCs), debris with a various size and artifacts also exist. Moreover, objects which cannot be identified due to the out-of-focus effect are also present. So, the algorithm should detect the WBCs, as many as possible while retain the low number of false detection. We found that our segmentation using multi-gray scale image is capable of detecting WBCs in bright field images with a high sensitivity, 95.4%. In contrast, the given %PPV is 72.7% which is not sufficient. Hence, re-segmentation step was developed in order to eliminate some false detection. We used FCM clustering to deal with this segmentation problem since it is the effective technique for gathering the similar data. Then, the cluster and ROI was select by the proposed algorithm. The result after applying re-segmentation show that a %PPV vastly increased to 89.2% while sensitivity slightly decreased to 92.90%.

The comparison result between WBCs segmentation before- (Fig.4.1c) and after-applying re-segmentation (Fig.4.1c) is shown in Fig.4.1. We found out that either applying multi-gray scale segmentation alone or with re-segmentation can correctly detect both clearly-seen (Fig.4.1 (top)) and ill-defined boundary cells (Fig.4.1 (bottom)) but the FCM clustering achieves more accurately segmentation. This accurate segmentation benefits for providing a certain region of cells in fluorescence images.

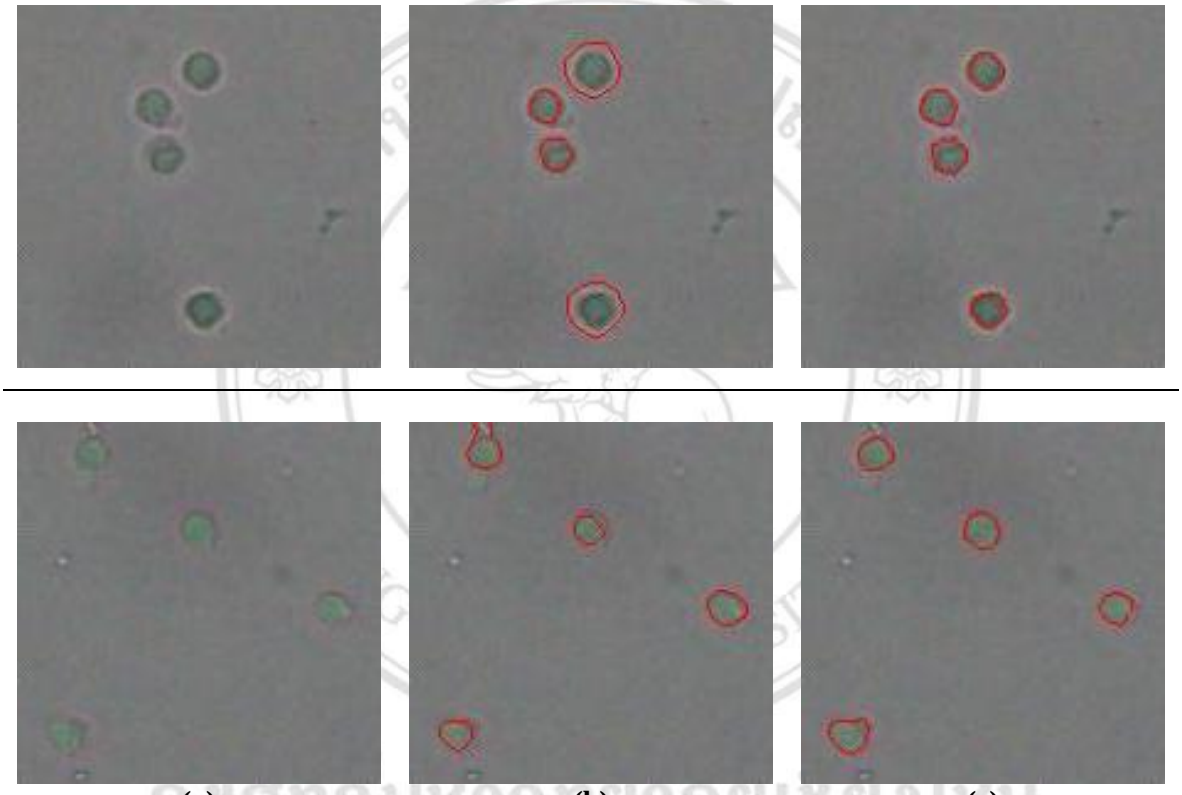

Figure 4.1 Comparison between before (b) and after (c) re-segmentation on clearly-seen (top) and ill-defined boundary cells (bottom).

The comparison between result of our WBCs detection method and the result drawn by expert is shown in Fig.4.2. The result obtained from expert was drawn with green color (Fig 4.2b) and algorithm result was drawn with red color (Fig.4.2c). Our algorithm shows the capability to detect all WBCs in the typical scene with a very accurate segmentation compared to ground truth (Fig. 4.2 (top)). Besides, groups of cells in the difficult scene are detected correctly (Fig. 4.2 (middle)). Also, cells form in a small cluster can be detected (Fig. 4.2 (bottom)). Furthermore, besides of background,

the false detection occurred from rough content debris (Fig 4.3a) and RBC (Fig 4.3b) are apparently gone.

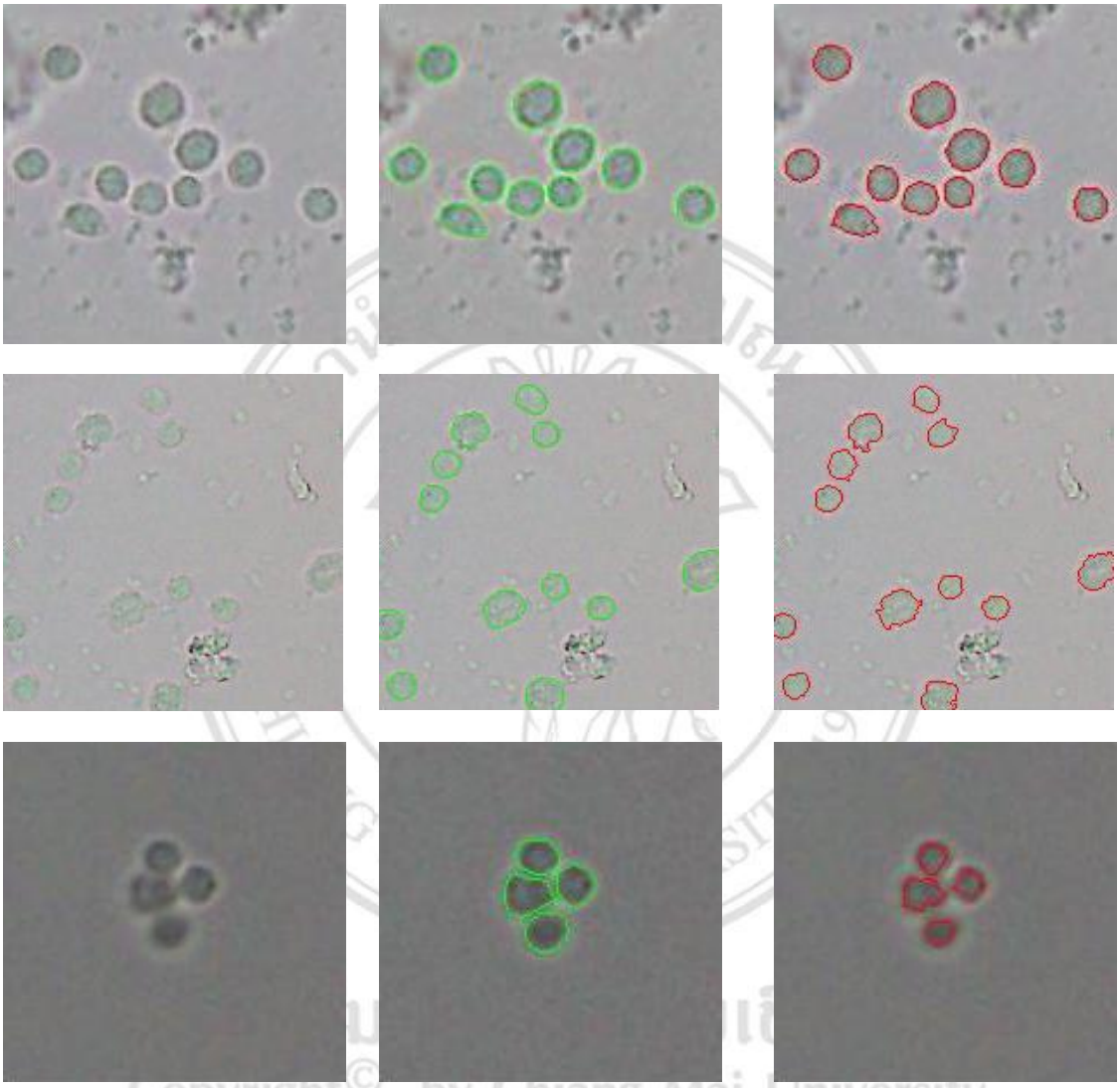

(a) **(b)** **(c)**

Figure 4.2 WBCs detection result (a) Group of cells in various scenes (b) Expert's result (c) Proposed algorithm result.

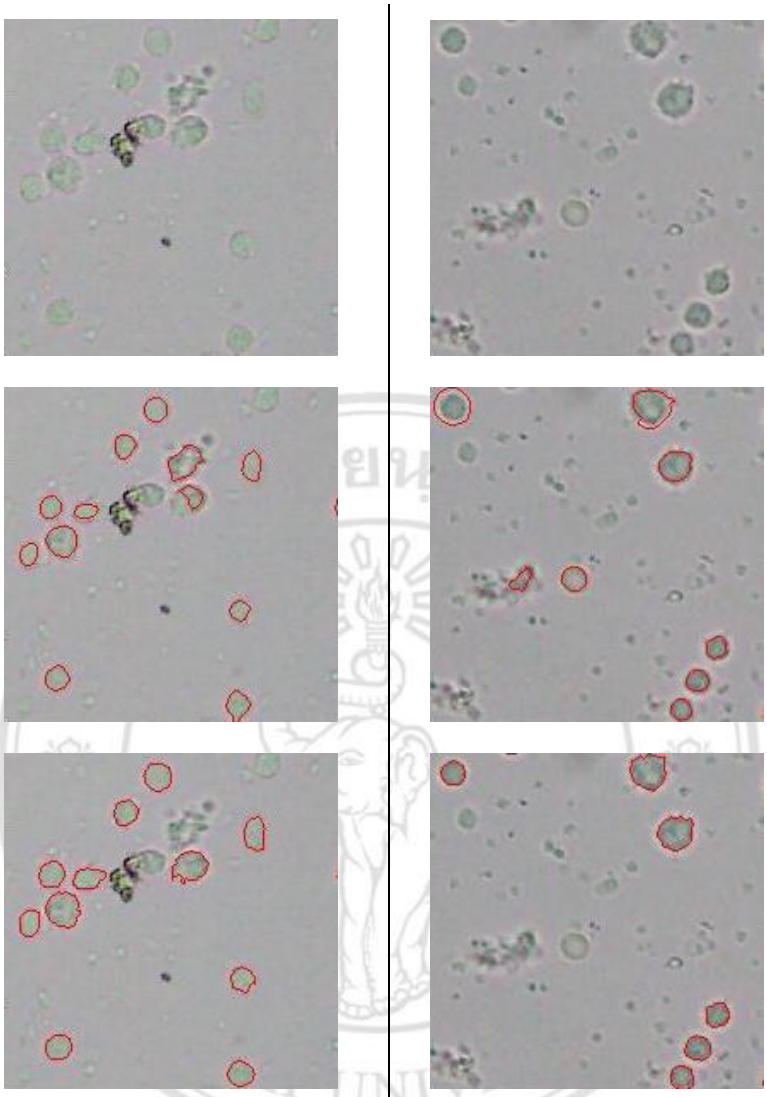

(a) **(b)**

Figure 4.3 Before (middle) and after (bottom) re-segmentation for (a) debris elimination (b) RBC elimination.

Moreover, we evaluated our approach with the additional opinion from other 2 experts in order to reduce resulting bias. We found out that the number of WBCs in our data set vary from 3663, 3438 and 3511 cells counted by expert 1, 2 and 3 respectively. Also, the counted WBCs by 3 experts are different for more than 100 cells. However, our proposed method compared to 3 experts yielded a good result with 93.32% of average sensitivity and 86.81% of average PPV as shown in Table 4.1.

Table 4.1 Result of WBCs detection algorithm compared to 3 experts.

Expert	Number of WBC (cells)	%PPV	%Sensitivity
1	3663	89.26	92.90
2	3438	85.54	93.33
3	3511	85.65	93.72
Average	3537	86.81	93.32
SD	114.79	2.12	0.41

However, the false positives which means non-WBCs are found still occur. For example, the blurred cells are pointed by the arrows (Fig 4.4a). 2 out of 3 experts said they were WBCs which means the opinion of the experts are not in the same way for this case. Also, some smooth-content debris (Fig.4.4b) whose content is homogenous cannot be discarded since their basic characteristic matches our rules. Smooth-content debris present the clearly-seen boundary and homogeneous content which can be easily distinguish from background by FCM clustering. Although their shape is far from circle, using the parameter roundness alone is ineffective for distinguishing the debris from the WBCs. In fact, if thresholding value of roundness was assigned close to 1, the debris will be discarded. However many WBCs in our data have ill-defined boundary caused poor segmented result. So, the thresholding value was empirically set lower to detect cells as many as possible in order to increase the opportunity to detect CD4+ lymphocytes in fluorescence images.

Likewise, false negative which means the missed detection are caused by debris attached cells which is hard to detect. The debris attached cells in Fig 4.5 had gone after cluster selection step. The cluster selection algorithm chooses the interested cluster based on assuming that cell locate on the middle of the cropped image. We found out that this assumption gave an incorrect solution for this case.

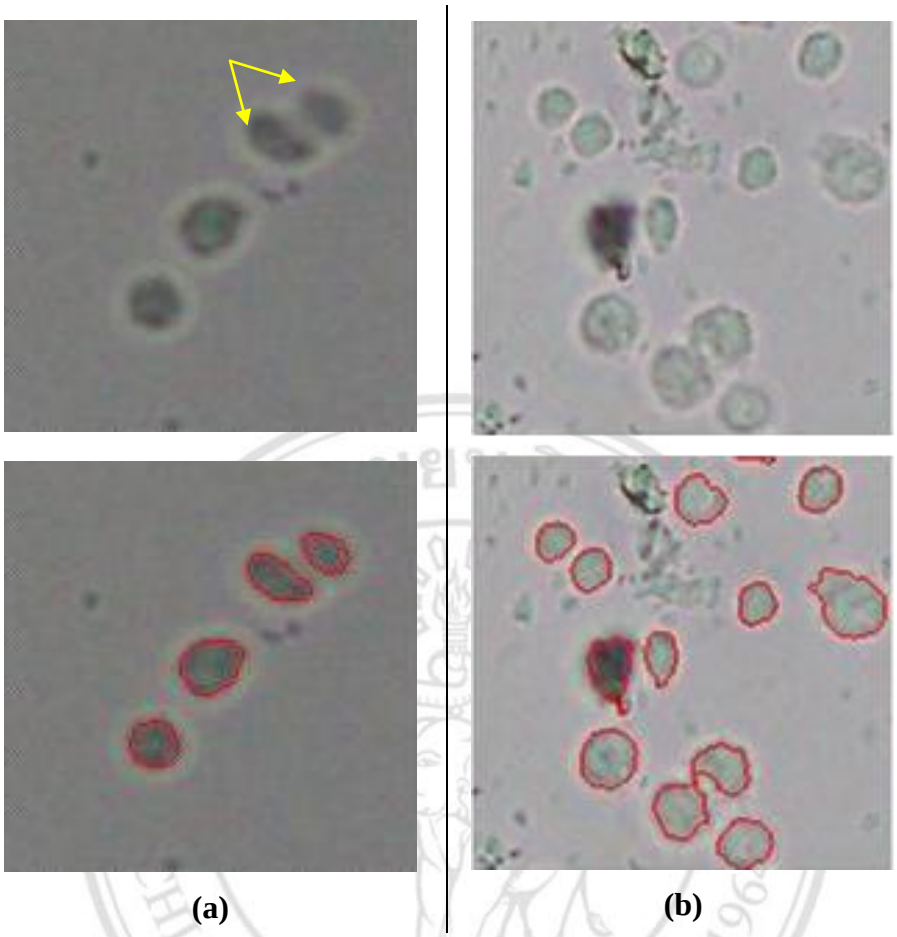

Figure 4.4 Example of false positives detection. (a) Blurred cell (b) Smooth- content debris.

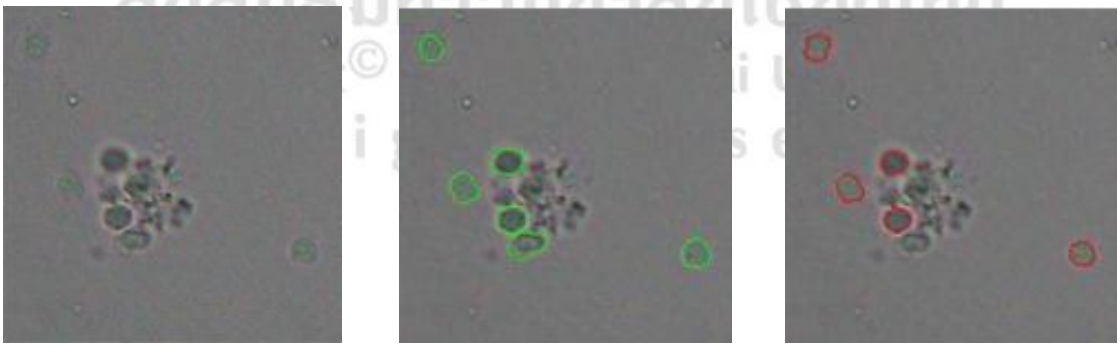

Figure 4.5 Example of false negative detection. (a) Cells attached debris scene (b) Expert's drawn (c) Missed detection cell.

4.2 CD4+ Lymphocyte Detection and Counting

The CD4+ lymphocytes are counted by the imbricated area among three images: bright field, green fluorescence and red fluorescence images. The performance of this step was evaluated by using the ROC curve. The ROC curves of green and red fluorescence image are generated separately since the illuminance of PE and FITC dyes are too much different. Red fluorescence from PE dyes has a higher intensity than green fluorescence from FITC dyes because it was performed by indirect staining where the fluorescence signal is higher. According to the ROC curve, true positive rate (TPR) and false positive rate (FPR) are determined at each thresholding value $T_{fluorescence}$ which range from 0 to 255.

The experiment evaluated by comparing proposed algorithm's result to the experts. The detection performance was evaluated by ROC curves of green and red fluorescence images in Fig 4.6. The thresholding value where nearest to the point which TPR=1 and FPR = 0 has shown the best TPR and FPR of the method. The best %TPR and %FPR obtained from ROC curve of green florescence images using the expert 1 as the ground truth are 93.4 and 8.3 respectively and from ROC curve of red florescence images using the expert 1 as the ground truth are 90.7 and 6.5 respectively.

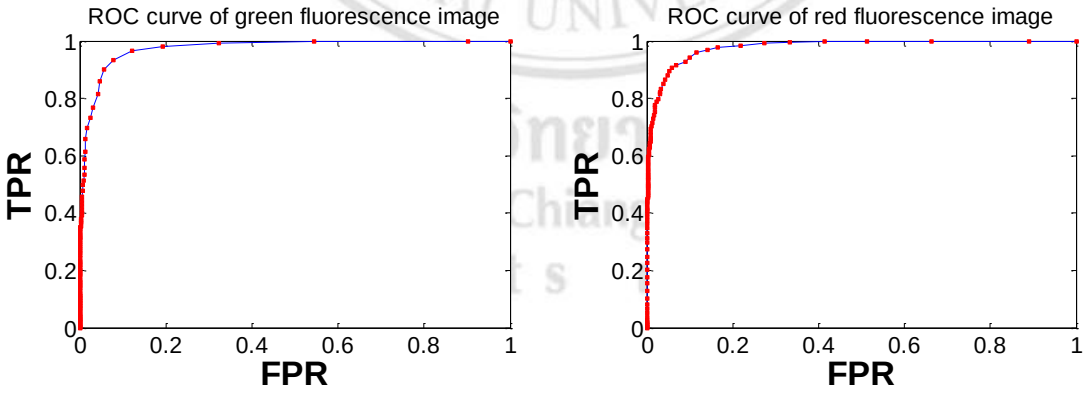

Figure 4.6 ROC curves of the proposed method using expert 1's opinion as ground truth.

Then we applied a pair of T_g and T_r as shown in Table 4.2 to test the CD4+ lymphocyte counting performance. The sensitivity and PPV are used to evaluate this test. The performance of a pairs T_g =12 and T_r =28 evaluated by using expert 1 as a ground truth, gave a 86.8% of sensitivity and 87.4% of PPV. The comparative result between the proposed algorithm and expert 1 using three pairs of thresholding value T_g =12 and T_r =26, T_g =12 and T_r =28, T_g =12 and T_r =30, are shown in Fig. 4.7. Almost all CD4+ lymphocytes are counted correctly, when compared to the expert's results (Fig. 4.7b). However, there are 2 false positives occurred which are indicated by the arrow (Fig. 4.7c and 4.7d). The false.positive at the right side of the image is also found because of the intensity diffraction effect. Since this cell located between the true positive cell and the debris which also has a red color, the intensity in this area is higher than the background. However, it disappeared after increasing T_r = 30 (fig.4.7e). Another false positive at the left side of the image represent a poorly certain boundary, also the intensity in green fluorescence image is fairly visible. However, this occurred false positive was said it was a CD4+ positive lymphocyte by the opinion of expert number 3.

In the green fluorescence images, using both R and G channels are effective in detecting CD4+ lymphocytes whose color is yellow. The multi-scale top-hat transform is effective in enhancing the positive cells with various sizes corresponding to the size of structure element used. Also, positive cells whose appearance is poor can also be detected. However, selecting the range of structure element should be careful since the larger the structure element, the higher the background appear.

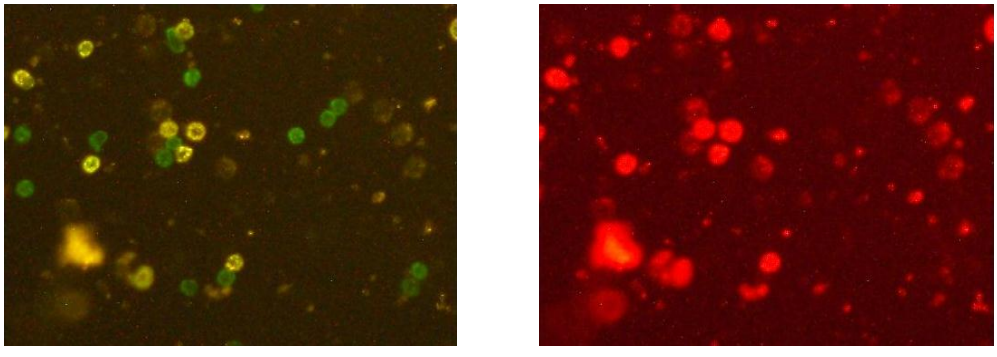

(a)

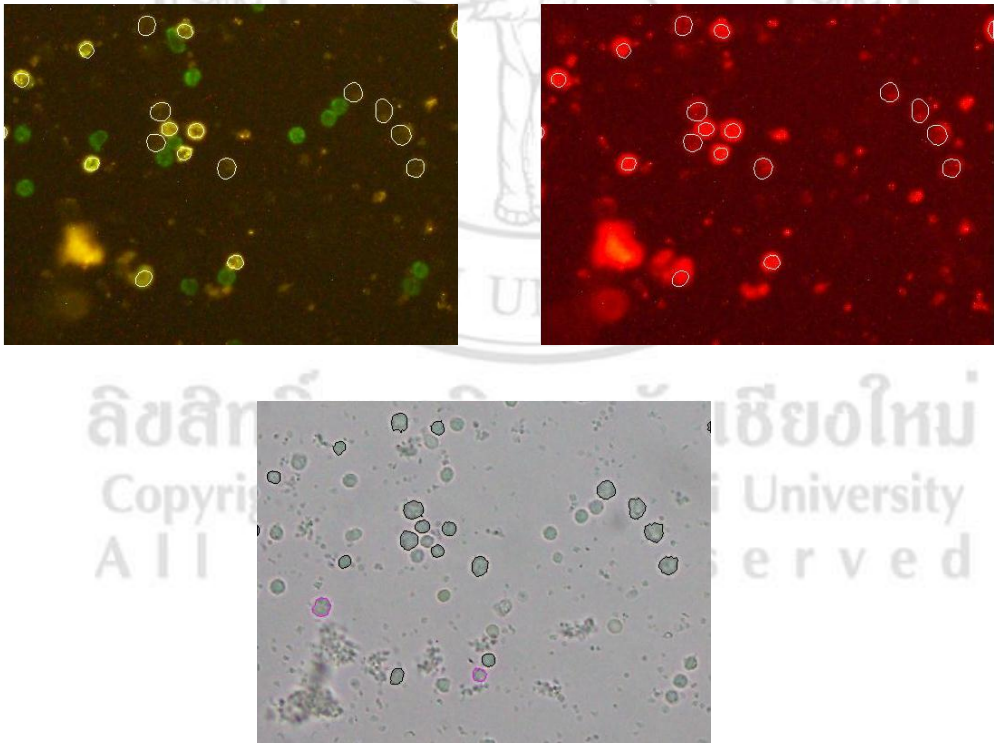

(b)

Figure 4.7 Results of CD4+ lymphocyte counting by applying 3 pairs of T_g and T_r to the image series. (a) Original images (b) Ground truth from expert 1 (c) T_g = 12 and T_r = 26 (d) T_g = 12 and T_r = 28 (e) T_g = 12 and T_r = 30 (cont.)

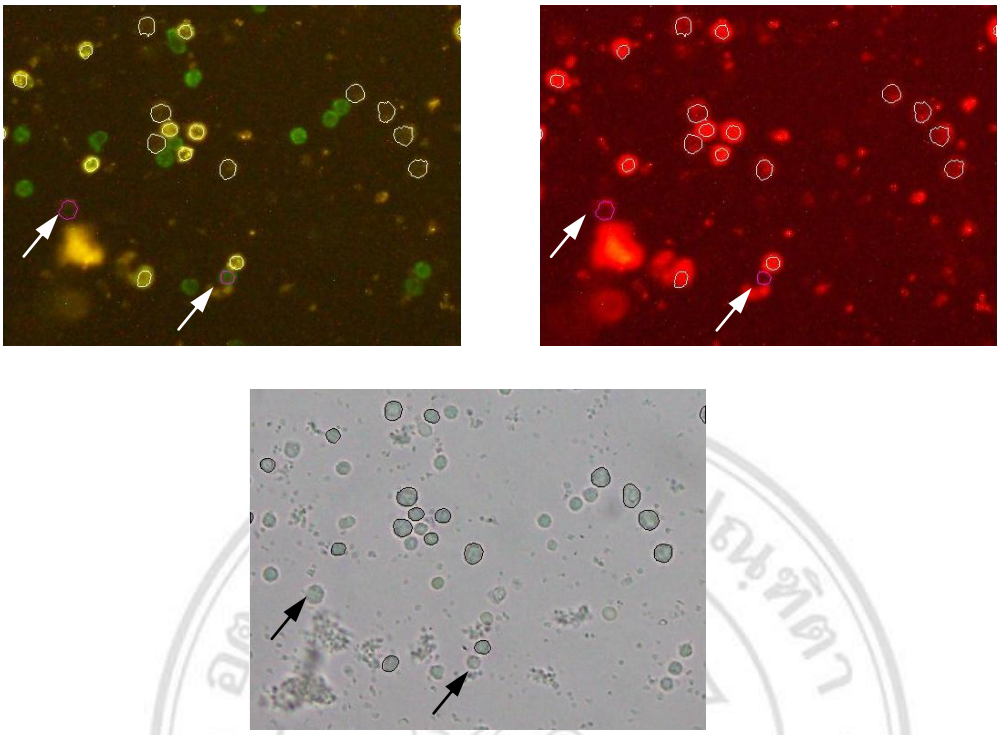

(c)

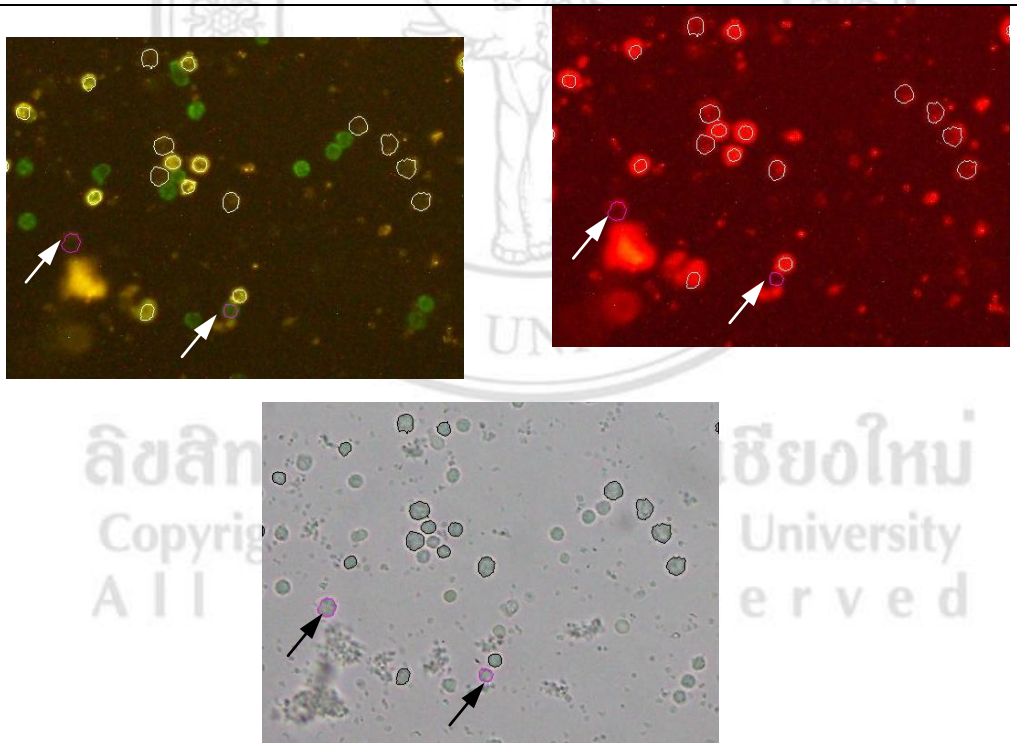

(d)

Figure 4.7 Results of CD4+ lymphocyte counting by applying 3 pairs of T_g and T_r to the image series. (a) Original images (b) Ground truth from expert 1 (c) T_g = 12 and T_r = 26 (d) T_g = 12 and T_r = 28 (e) T_g = 12 and T_r = 30 (cont.)

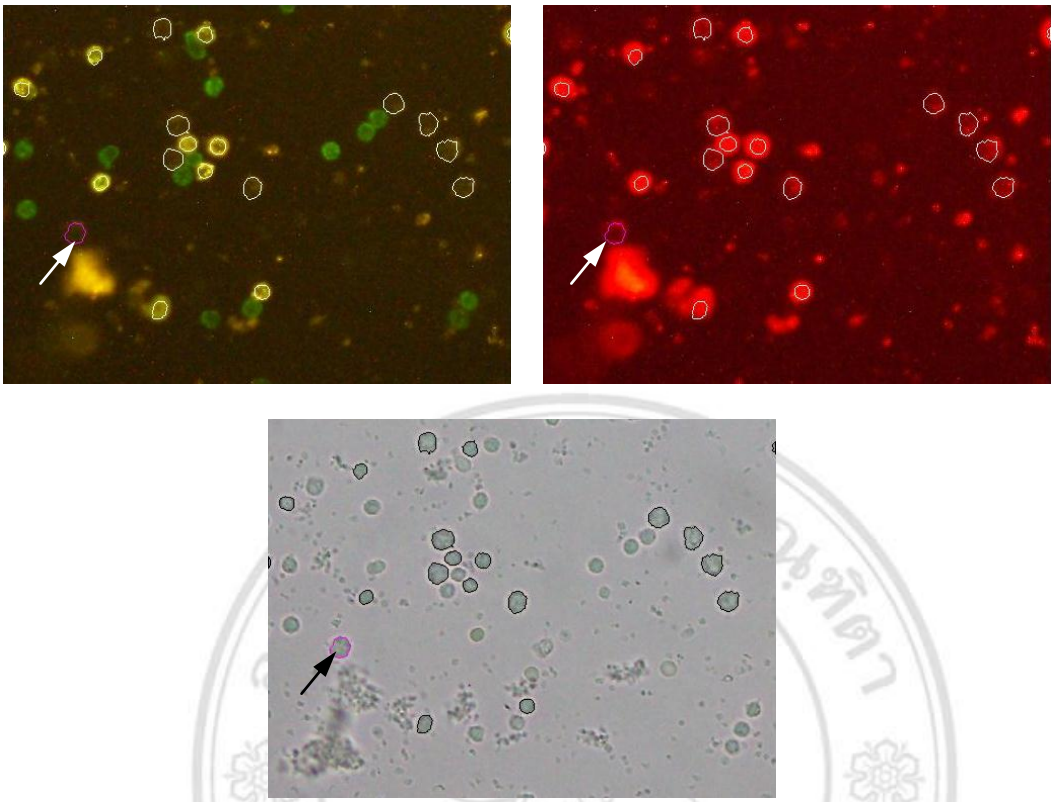

(d)

Figure 4.7 Results of CD4+ lymphocyte counting by applying 3 pairs of T_g and T_r to the image series. (a) Original images (b) Ground truth from expert 1 (c) T_g = 12 and T_r = 26 (d) T_g = 12 and T_r = 28 (e) T_g = 12 and T_r = 30 (cont.)

The additional evaluation by ROC curve using the other 2 experts as ground truth are shown in Fig. 4.8 and 4.9. The optimal thresholding of each ROC curve from 3 experts are shown in the Table 4.3. The result shows the various optimal thresholding values depending on the expert opinion. The result from expert 2 where T_g=20 and T_r =36, gave 82.6 and 81.5 of a sensitivity and a PPV. The result from expert 3 where T_g=14 and T_r =28 are equal to 77.34 and 84.85 of a sensitivity and PPV, respectively. Then we applied a pair of thresholding value to every image in data set in order to count CD4+ lymphocyte. The result show a good performance when evaluated by experts 1 and 2 but the sensitivity of the result obtained from expert 3 is lower than the rest. However, it must be denoted here that there is the high variation among the opinions of each expert which can be express by the overall number of manual detected cells in data set. For cells which are positive in green fluorescence images, manual counting results

from expert 1, 2 and 3 are 2741, 2392 and 2693 cells, respectively. For cells which positive in red fluorescence images, manual counting results are 1669, 1381 and 1818 cells, respectively. For manual CD4+ lymphocytes counting, which positive for both colors are 1610, 1215 and 1615 cells, respectively. The different of manual counting of positive cells in green, red and both green and red fluorescence images are 189, 222 and 229 cells, respectively.

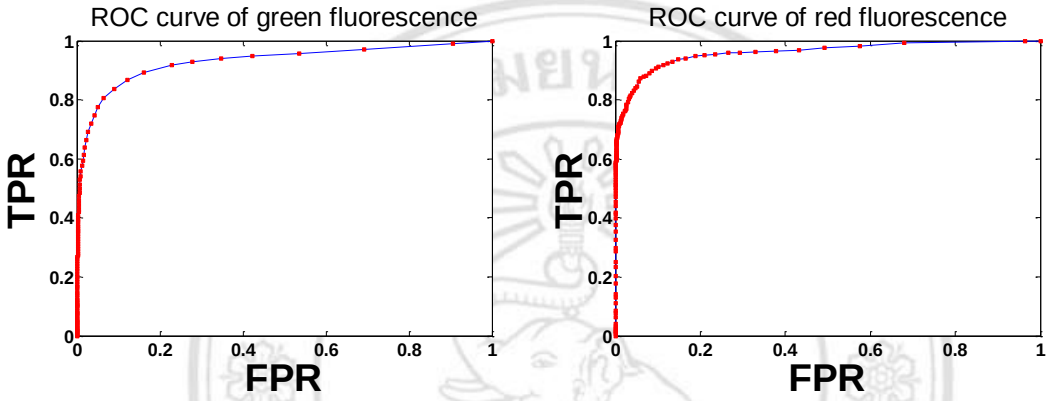

Figure 4.8 ROC curves of the proposed method using expert 2's opinion as ground truth.

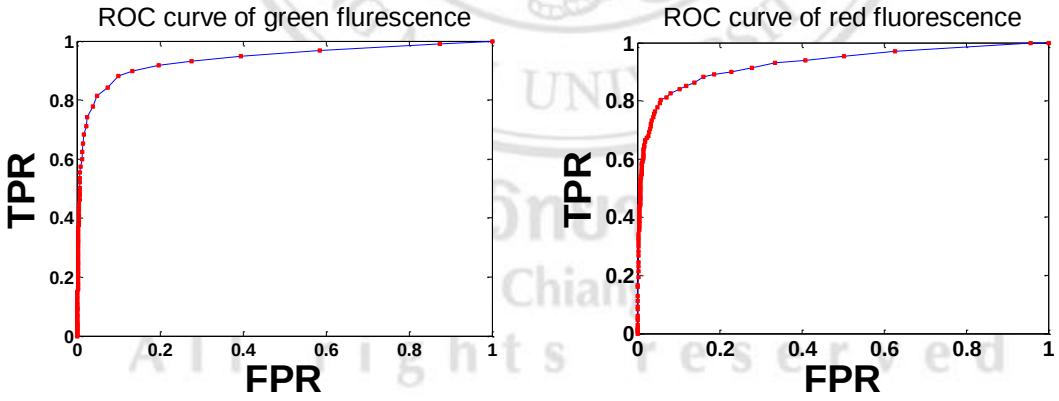

Figure 4.9 ROC curves of the proposed method using expert 3's opinion as ground truth.

Table 4.2 Thresholding value and performance from ROC curves.

Expert	**ROC of CD4+ lymphocyte detection**			
	Optimal threshold		**%TPR**	**%FPR**
1	T_q	12	93.4	8.3
	T_r	28	90.7	6.5
2	T_q	20	83.8	9.0
	T_r	36	91.1	10.0
3	T_q	14	88.0	10.0
	T_r	28	81.3	8.2

Table 4.3 Result of CD4+ lymphocyte counting performance using the thresholding value from ROC curves.

Expert	**Threshold**		**% Sensitivity**	**% PPV**
	T_q	T_r		
1	12	28	86.8	87.4
2	20	36	82.6	81.5
3	14	28	77.3	84.8

Moreover, the illumination variation among the different fluorescence images is high, so using a same thresholding value for all fluorescene images is probably ineffective. It require a better practice for reducing the variation of intensity between each image than a simple background subtraction. In another way, the optimal thresholding value should be applied individually. Similar to the diffraction of the fluorescence light, which causes the false positive, is quite difficult in this study. This characteristic is highly visible when the cells are strongly positive especially for red color. Besides of blurred boundary, the region of spot is larger than its actual size. Also, the intensity of surrounded pixels is increased. This effect should be intensively taken into account when cells were more adhered. Besides, the remaining small precipitate

dyes can cause the false positive when it lies over the region belonging to cell. The false positives caused by diffraction effect and small precipitate dyes cannot be discarded by determining the overlapping area alone but the good results should rely on the good thresholding value which provides the satisfaction of experts.

Furthermore, one difficulty which effect the performance of our proposed algorithm is cell shifting. The characteristic of cell shifting is that the cell in one image shifts from that position in other images in the associated scene. This effect is caused by image acquisition and hard to control because cells suspended in the solution occasionally float during switching among bright field, green and red fluorescence imaging. Although the switching does not take too long, it does not fast enough. Using the multi-band filter to simultaneously capture green and red florescence image might help reducing the cell shifting effect but it still occur when switching between bright field and florescence imaging. In this study, we assume that CD4+ lymphocyte should be in the same location in the corresponding images without shifting effect occurs. In fact, mild-shifted cells (Fig.4.10a) which show more than 50% of overlapping area among bright field, green and red fluorescence can be detected by our proposed algorithm. However, cells which completely shift (Fig.4.10b) without presenting the overlapping area cannot be detected. So, to increase the algorithm sensitivity, solution of cell shifting problem should be taken into account.

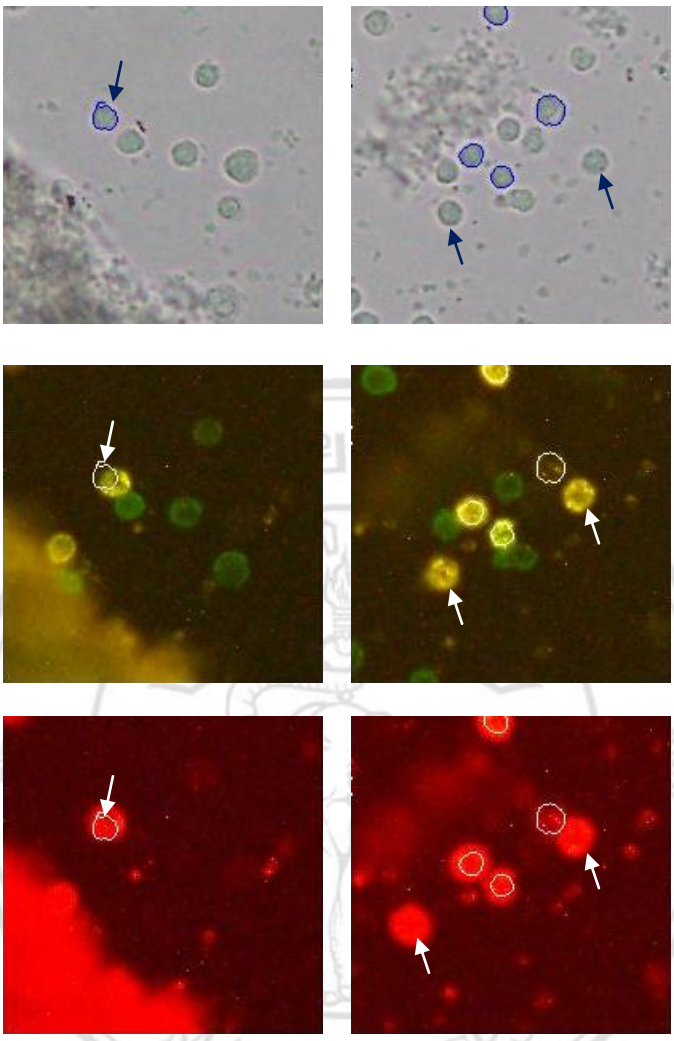

(a) **(b)**

Figure 4.10 Cell shifting. (a) Mild-shifted cell (b) Complete-shifted cells.